Proton acceleration from near critical density foam targets using the Vulcan Petawatt laser

L. Willingale, S. P. D. Mangles, S. R. Nagel, C. Bellei, A. E. Dangor, M. C. Kaluza, C. Kamberidis, S. Kneip, Z. Najmudin, P. M. Nilson, A. G. R. Thomas and K. Krushelnick
The Blackett Laboratory, Imperial College London, Prince Consort Road, London, SW7 2BW, UK

R. J. Clarke and R. Heathcote
Central Laser Facility, CCLRC Rutherford Appleton Laboratory, Chilton, Didcot, Oxon., OX11 0QX, UK

W. Nazarov
University of St. Andrews, Fife, KY16 9ST, UK

N. Lopes
GoLP, Instituto Superior Tecnico, Lisbon, Portugal

K. Marsh
Department of Physics and Astronomy and Electrical Engineering, UCLA, Los Angeles, California 90095, USA

Main contact email address louise.willingale@imperial.ac.uk

Introduction

There has been extensive research into laser generated multi-MeV proton beams since the development of high intensity (>10^{18} Wcm^{-2}) lasers. The properties of these charge-neutralised laser-produced proton beams are a small transverse emittance, small virtual source size, large total charge and good beam quality. Qualities such as these make them interesting for possible applications such as proton radiography, isochoric heating, cancer therapy and even as possible injectors for higher energy accelerators.

Previous measurements have looked at protons accelerated from solid (overdense) targets, which usually originate from contaminants on the target surface. A hot electron beam is created by the laser interaction with the target. Charge separation caused by the ponderomotive force of the laser can accelerate protons from the front of the target. The electron beam propagates through the target and exits into the vacuum. This sets up a large space charge field at the rear of the target, which is able to accelerate protons and ions from the target rear surface. The balance between the front and rear acceleration mechanisms and the efficiency of the acceleration is determined by laser pre-pulse level, intensity and pulse length and target material and thickness. Simple theoretical scaling laws[1] show that the maximum proton energy should increase with higher fast electron temperatures, T_e. It is usual that much higher fast electron temperatures can be reached in underdense plasmas[2] than in the solid target (overdense) interactions. Ion beams accelerated in the forward direction from underdense targets have recently been observed[3]. The increased electron temperature from underdense plasma enables the acceleration mechanism to overcome the low ion density. It was observed that the ion acceleration improved with density.

Absorption of laser energy in laser-solid interactions into the plasma is most efficient at densities near the critical density, the density at which incident light is reflected for normal incidence. This is also of significant interest to laser plasma studies.

Presented in this report are the preliminary results from a Vulcan Petawatt experiment in which near critical density foams were used at the target. The effect of the combination of the more efficient electron acceleration with the propagation of the laser through the target with the high proton and ion densities is investigated.

Experimental set up

The experiments were performed using the Vulcan Petawatt laser at the Rutherford Appleton Laboratory. The laser wavelength is centered at 1.055 μm and the average FWHM pulse length was 570 fs. The beam is focused by an f/3 off axis parabolic mirror to a FWHM intensity vacuum focal spot diameter of 5 μm to give a maximum peak vacuum intensity of 7×10^{20} Wcm^{-2} in this investigation. This corresponds to a peak normalized vector potential of $a_0 \sim 24$.

The low density foam targets were produced using the in situ polymerization technique. The CHO foams were mounted in washers 250 μm thick and examples of the foam structure are shown in figure 1. Table 1 shows the different densities available and the maximum electron density that a fully ionized foam would produce. The non-relativistic critical density for this wavelength is $n_c = 10^{21}$ cm^{-3}. However at such high intensities the plasma electrons will be relativistic and the effective critical density is considerably higher. The laser is linearly polarised so the average relativistic critical density, $n_{c\gamma} = \langle\gamma\rangle n_c$, where the time averaged gamma factor, $\langle\gamma\rangle = (1 + a_0^2/2)^{1/2}$. For an $a_0 = 24$ for linearly polarised light, this gives a $n_{c\gamma} = 17n_c$.

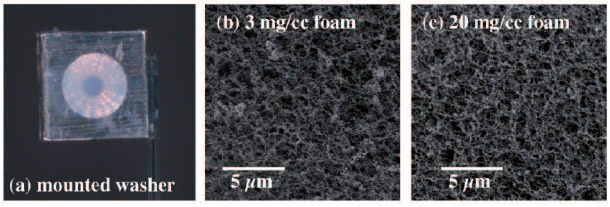

Figure 1. (a) The foams were mounted in washers of 250 μm thickness and (b) and (c) are high magnification images showing the structures in the low density foams (courtesy of C. Spindloe, target fabrication, CLF). The 5 μm scale is similar to the focal spot size.

Foam density (mg/cm^3)	Maximum n_e (cm^{-3})	Maximum n_e/n_c
3	9×10^{20}	0.9
5	1.5×10^{21}	1.5
15	4.5×10^{21}	4.5
20	6×10^{21}	6
45	1.5×10^{22}	15
100	3×10^{22}	30

Table 1: The foam densities and the corresponding maximum electron number densities assuming a fully ionized plasma. The non-relativistic critical density is n_c.

The main diagnostics were an on axis electron spectrometer, Thomson ion spectrometers at 2° and 45°, copper activation stacks and burn paper and scattered ω light imaging to look at the transmitted laser light through the foams. The low density foam targets were shot at 0° incidence, apart from one which was set at 10° incidence to look at the relative direction of the proton beam. There was a comparison shot onto a 10 μm thick mylar target which was shot at 45° incidence. The geometries for the targets and diagnostics are shown in figure 2. It was not possible to field all of the diagnostics simultaneously as the activation stacks blocked the target normal spectrometers and burn paper so two shots were needed for complete data sets for each foam density.

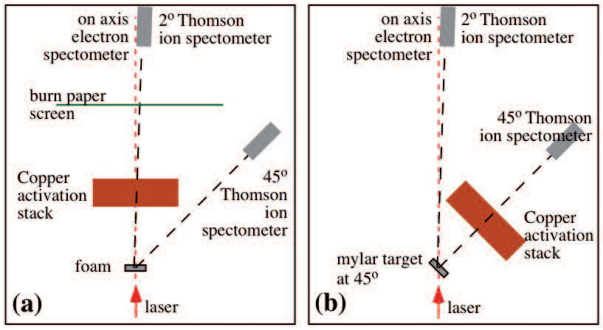

Figure 2. Experimental set up for (a) the foam targets and (b) the mylar targets.

Experimental results

The first comparison between the solid mylar target and the foam targets is to look at the electron spectra, which is shown in figure 3. For the same spectrometer magnet settings, there were high energy electron spectra for all of the foam targets, however for the mylar target the energies were below the energy threshold of the spectrometer. The bump at around 60 MeV in the spectra is due to a shielding artifact and is not a real part of the electron spectra.

The copper activation stack can be used to measure the proton spectra. However, care has to be taken when analysing the data because protons are not the only source of nuclear reactions. For the foam shots, it has been seen that electrons are accelerated up to high energies and number. This gives a high probability for gamma reactions occurring in the stack since the electron beam will pass through it as well as protons for the foam shots. By considering the cross sections for the possible reactions and the half-lives of the products of the largest cross section reactions it is possible to calculate a proton spectra. The product ^{63}Zn only has large cross-sections for incident protons and ^{63}Zn has a half-life of about 40 minutes. By recording the activity of a piece of copper at different times after the shot and fitting a decay curve to these measurements for different product half-lives, an estimate of the initial number of each product can be found. The initial number of ^{63}Zn atoms per μm of copper against the depth into the stack is shown in figure 4.

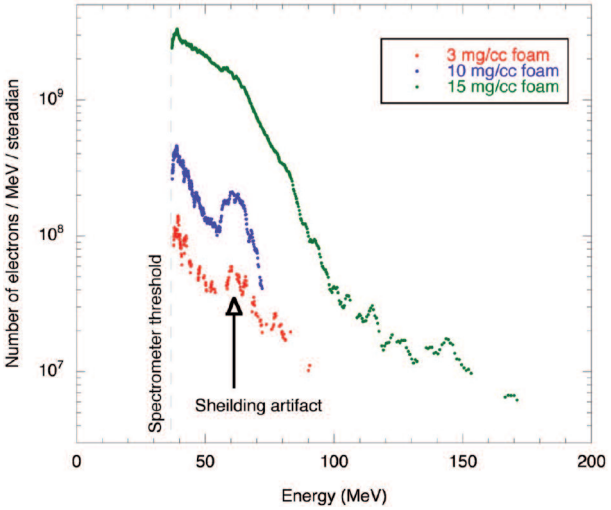

Figure 3. The on-axis electron spectra for three different density foam shots. The electron spectra for the mylar target was below the spectrometer threshold.

The proton beam profile is recorded on radiochromic film pieces interspersed in the copper activation stack. It is sensitive to all ionizing radiation but protons produce the largest signal. Figure 5 shows the radiochromic film pieces from the same stacks. The energies (in Joules) shown under the target labels are the on target laser energies. On the left, the proton energies stopped in that layer of radiochromic film are shown. The 3mg/cc target was aligned ~ 10° off axis for this shot and the proton emission was off axis by this amount. This shows that the proton

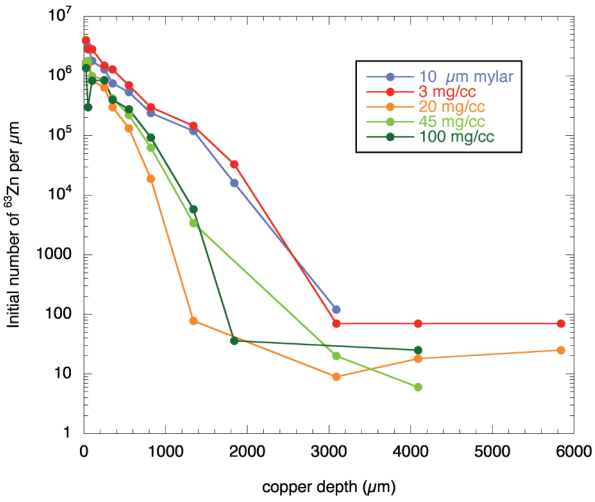

Figure 4. The initial ^{63}Zn atoms per μm as a function of depth through the stack for different targets. The ^{63}Zn activation is due to incident protons.

acceleration is in the target normal direction for the foam targets in the same way that it is for the solid targets. The wispy horizontal/vertical cross features on some of the radiochromic films has been observed before[4] and could be due to the movement of plasma from the front of the target to the rear of the target[4] or due to emission from the edges of the target[5]. The washers are small (1 mm by 1mm by 0.25 mm) and will therefore be particularly prone to this. The proton beam divergence for protons ≥ 22 MeV the beam divergences are shown at the bottom of figure 5.

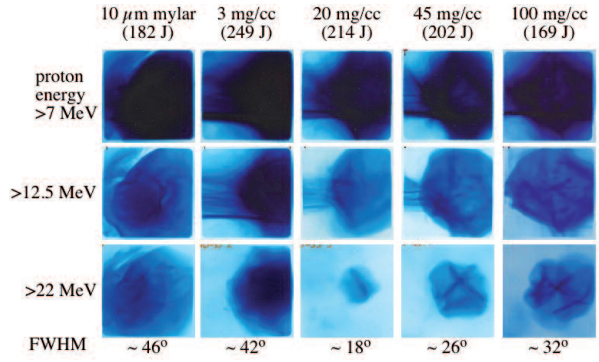

Figure 5. Radiochromic film from different depths in the stack (corresponding to different proton energies, shown on the left) for different targets. The labels at the bottom show the approximate FWHM divergence of the proton beam at ≥22 MeV

To investigate the transmission of the laser light through the foams a combination of burn paper and imaging the scattered laser light at (was used and these results are shown in figure 6. The scattered image labeled '2 minute shot' is from a low power shot for which it is estimated that there would be 100 mJ of energy on target. The scattered light images show that the light at ω is still collimated so it is the laser light that is being observed, not transition radiation from the plasma. Using 100 mJ of laser energy to calibrate the signal of scattered light and relate that to the transmitted laser energy through the foams gives 75-80% transmission. However considering the burn paper data this seems high compared with the burn paper signal. Therefore, it is likely that the energy on target for a 2 minute shot is more in the range of 10 - 50 mJ.

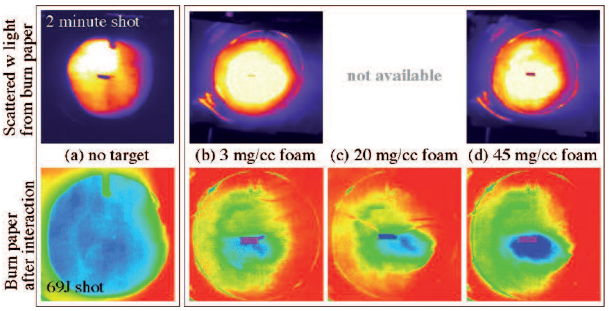

Figure 6. The top pictures show scattered ω light from the burn paper during the shots (not on same scales). The lower images are of the burn papers (background corrected, on same scale).

Conclusion

The foam targets produce higher energy and temperature electron beams than the comparison solid targets. From the copper activation measurements, the lowest density foam (3 mg/cm^3) produced a similar activation measurement compared to the solid mylar target. However, the laser energy for the 3 mg/cm^3 foam shot was higher. The proton beam profiles for the foam targets all had a smaller angular divergence than the solid target, but the numbers were down. A significant proportion of the laser light has been observed to be transmitted through the foams, estimated to be 3% - 30% of the incident laser energy.

Further work will include numerical modeling of the interaction to look at the laser propagation, energy absorption and the electron acceleration in near critical density plasmas.

Acknowledgements

The authors gratefully acknowledge the assistance of the Central Laser Facility staff at the Rutherford Appleton Laboratory in carrying out this work. The UK Engineering and Physical Sciences Research Council (EPSRC) supported this research.

References

1. P. Mora, *Phys. Rev. Lett,* **90**, 185002 (2003)
2. S. P. D. Mangles *et al*., *Phys. Rev. Lett,* **94**, 245001 (2005)
3. L. Willingale *et al*., *Phys. Rev. Lett.* **96** 245002 (2006)
4. E. L. Clark, *PhD Thesis*, University of London (2001)
5. F. N. Beg *et al*., *Appl. Phys. Lett.* **84**, 2766 (2004)